JACS
JOURNAL OF THE AMERICAN CHEMICAL SOCIETY
Cite This: J. Am. Chem. Soc. 2019, 141, 5640−5644
Communication
pubs.acs.org/JACS

Rotational Cluster Anion Enabling Superionic Conductivity in Sodium-Rich Antiperovskite Na_3OBH_4

Yulong Sun,[†] Yuechao Wang,[‡] Xinmiao Liang,[§] Yuanhua Xia,[∥] Linfeng Peng,[†] Huanhuan Jia,[†] Hanxiao Li,[‡] Liangfei Bai,[∥] Jiwen Feng,[§] Hong Jiang,*[,‡] and Jia Xie*[,†]

[†]State Key Laboratory of Advanced Electromagnetic Engineering and Technology, School of Electrical and Electronic Engineering, Huazhong University of Science and Technology, Wuhan, Hubei 430074, China

[‡]Beijing National Laboratory for Molecular Sciences, College of Chemistry and Molecular Engineering, Peking University, 100871 Beijing, China

[§]State Key Laboratory of Magnetic Resonance and Atomic and Molecular Physics, National Center for Magnetic Resonance in Wuhan, Wuhan Institute of Physics and Mathematics, Chinese Academy of Sciences, Wuhan, Hubei 430071, China

[∥]Key Laboratory of Neutron Physics and Institute of Nuclear Physics and Chemistry, China Academy of Engineering Physics, Mianyang, Sichuan 621999, China

Supporting Information

ABSTRACT: Sodium superionic conductors are keys to develop high safety and low cost all-solid-state sodium batteries. Among developed sodium ionic conductors, antiperovskite-type ionic conductors have attracted vast interest due to their high structural tolerance and good formability. Herein, we successfully synthesize Na_3OBH_4 with cubic antiperovskite structure by solid-state reaction from Na_2O and $NaBH_4$. Na_3OBH_4 exhibits ionic conductivity of 4.4×10^{-3} S cm^{-1} at room temperature (1.1×10^{-2} S cm^{-1} at 328 K) and activation energy of 0.25 eV. The ionic conductivity is 4 orders of magnitude higher than the existing antiperovskite Na_3OX (X = Cl, Br, I). It is shown that such enhancement is not only due to the specific cubic antiperovskite structure of Na_3OBH_4 but also because of the rotation of BH_4 cluster anion. This work deepens the understanding of the antiperovskite structure and the role of cluster anions for superionic conduction.

The demands in large-scale energy storage motivate the development of new energy storage technologies with low cost and high safety.[1,2] All-solid-state sodium batteries combining the low cost and high abundance of Na resources as well as the high safety feature of all-solid-state batteries are promising candidates.[3,4] Sodium superionic conductors are keys to develop such batteries. A variety of inorganic sodium superionic conductors have been reported.[5−14] Among these reported superionic conductors, oxides sodium superionic conductors have attracted broad attention in the battery community, due to their high chemical/electrochemical combability against Na metal.[5,15] However, traditional oxides, such as β-Al_2O_3 and NASICON family,[5−7] usually achieve the high ionic conductivity (>10^{-3} S cm^{-1}) via high temperature (~1000 °C) sintering process to decrease the grain-boundary resistances. Recently reported oxide lithium superionic conductors, antiperovskite $Li_3OCl_{1-x}Br_x$, are promising materials, since they exhibit not only high ionic conductivity (>10^{-3} S cm^{-1})[16] and good electrochemical stability[17,18] but also relatively low melting point (~280 °C),[16] which enables reducing the grain-boundary resistances at low temperatures.

The appearance of antiperovskite $Li_3OCl_{1-x}Br_x$ has also inspired the study on the sodium analogues. Antiperovskite Na_3OX (X = Cl, Br and I) have been successfully synthesized and also show low melting point (~250 °C).[19] Unfortunately, the optimized ionic conductivity of Na_3OX is 1.9×10^{-3} S cm^{-1} at 200 °C and 10^{-6}−10^{-7} S cm^{-1} at room temperature, which is much lower than that of the lithium analogues and cannot meet the application requirement (>10^{-4} S cm^{-1}). Although the optimized ionic conductivity is still low, it suggests the high structure tolerance of Na_3OX and possible chemical manipulation on ionic conductivity.[19]

Superhalogen cluster anions, such as BH_4, AlH_4 and BF_4, are potential choices to replace halogens for boosting the ionic conductivity, based on following considerations: (1) similar chemistry with halogens;[20] (2) larger radii for larger channel sizes;[21,22] (3) rotational motion of cluster anions promoting Na/Li conduction ("paddle-wheel" effect).[21,23] The low activation energy and high ionic conductivity have been predicted in some cluster anions based antiperovskite superionic conductors by density functional theory (DFT) calculations.[20−22] However, to the best of our knowledge, there is no experimental report on synthesis nor conductivity. Herein, we explore cluster anions based antiperovskite Na_3BX (B = O, S; X = BH_4, BF_4) sodium ionic conductors. Na_3OBH_4 with cubic antiperovskite structure is successfully synthesized by solid-state reaction from Na_2O and $NaBH_4$. Na_3OBH_4 exhibits the superionic Na conduction with ionic conductivity of 4.4×10^{-3} S cm^{-1} at room temperature (1.1×10^{-2} S cm^{-1} at 328 K) which is 4 orders of magnitude higher than that of antiperovskite Na_3OX (X = Cl, Br, I). The Na vacancies and the specific cubic antiperovskite structure are important for the high ionic conductivity. Both Neutron powder diffraction and

Received: February 14, 2019
Published: March 26, 2019

DOI: 10.1021/jacs.9b01746
J. Am. Chem. Soc. 2019, 141, 5640−5644

first-principles calculations reveal the rotation of BH_4 anion and its enabling effect on Na superionic conductivity.

Synthesis of Na_3BX (B = O, S; X = BH_4, BF_4) are attempted from Na_2O, Na_2S, $NaBF_4$ and $NaBH_4$ through one step solid-state reaction (eq 1). Figure 1 presents XRD pattern of as-

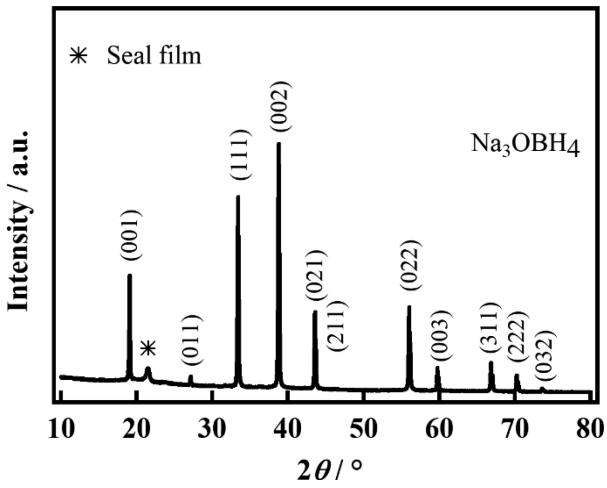

Figure 1. XRD patterns of synthesized Na_3OBH_4 with assigned Miller indices.

synthesized Na_3OBH_4. The diffraction peaks are assigned to antiperovskite-type Na_3OBH_4 phase, and no impurity peaks are observed in the XRD pattern. However, the synthesis of antiperovskite Na_3SBH_4 and Na_3SBF_4 fails and yields either starting materials or complex mixture (Figure S2). These results are somewhat consistent with the Goldschmidt tolerance factor which is an experiential indicator for the stability and distortion of the cubic antiperovskite structure. In this study, the Goldschmidt tolerance factor for nominal Na_3BX (B = O, S; X = BH_4, BF_4) can be given as

$$t = (R_{Na} + R_X)/\sqrt{2}(R_{Na} + R_B)$$

where R_{Na} is radius of Na^+, R_B is radius of O^{2-}/S^{2-} and R_X is radius of BH_4^-/BF_4^-. Anions and cations with $0.9 \le t \le 1$ are highly possible to form the cubic phases.[24] BH_4^- has the close ionic radius to that of Br^- (R = 1.96 Å,), and the t of Na, O and BH_4 is 0.90 (Table 1), which suggests the high ability of

Table 1. Goldschmidt Tolerance Factor for Na_3BX[a]

ions and ionic radius (Å)	t
Na(0.95), O(1.40), BH_4(2.03)	0.90
Na(0.95), S(1.84), BH_4(2.03)	0.76
Na(0.95), O(1.40), BF_4(2.43)	1.02
Na(0.95), S(1.84), BF_4(2.43)	0.86

[a]B = O, S; X = BH_4, BF_4.

Na_3OBH_4 to stabilize the cubic antiperovskite structure. Thus, we demonstrate a facile synthesis of phase-pure antiperovskite Na_3OBH_4, which could also be an alternative route to synthesize Na_3OX (X = Cl, Br, I).

$$Na_2B + NaX \rightarrow Na_3BX\ (B = O, S; X = BH_4, BF_4) \quad (1)$$

XRD data shows that there is no diffraction peak splitting resulted from small tetragonal or orthorhombic distortions from the cubic,[19] and the diffraction peaks are indexed to be the characteristic from typical simple cubic lattice. The Miller indices are assigned to each characteristic peak in Figure 1. The only one Na peak in solid state ^{23}Na NMR spectrum (Figure 2a) also suggests the cubic antiperovskite structure of

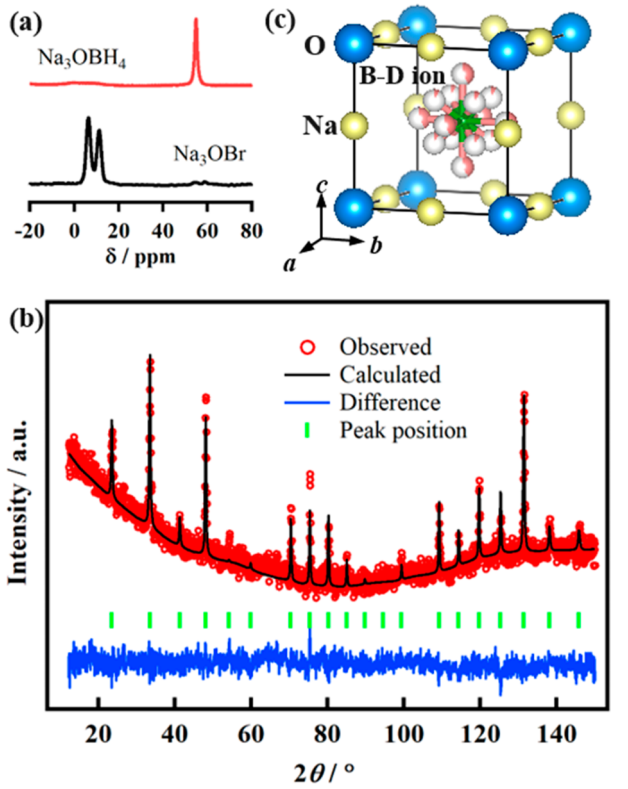

Figure 2. (a) Solid state ^{23}Na NMR spectra of Na_3OBH_4 and Na_3OBr. (b) Rietveld refinement plots of Na_3OBD_4 neutron powder diffraction at 300 K. (c) Crystal structure of Na_3OBD_4 derived from neutron powder diffraction Rietveld refinement.

Na_3OBH_4 without small tetragonal or orthorhombic distortions from the cubic. The B and H remain as BH_4 group in Na_3OBH_4 (Figure S3). Interestingly, from the ^{23}Na NMR results of Na_3OBr, there are at least two distinguishable Na sites in Na_3OBr, although Na_3OBr has been reported as cubic antiperovskite structure with only one Na site.

On the basis of above analysis, the structural information of Na_3OBH_4 is further investigated by Rietveld refinement of X-ray diffraction and neutron powder diffraction. Na_3OBH_4 crystallizes into $Pm\bar{3}m$ (221) space group. The cell parameter a from XRD Rietveld refinement is 4.63204 (1) Å (Table S1), which is slightly larger than that of Na_3OBr.[19] It is challenging to determine information of light atoms, such as B and H in the structure by XRD data. Due to the strong incoherent scattering of H, Na_3OBD_4 is synthesized and submitted to neutron powder diffraction for detailed structural analysis. The refined plots of neutron powder diffraction and the structure of Na_3OBD_4 are shown in Figure 2b,c, which reveal vacancies at Na sites (Table S2). D occupies two sites, 6*f* and 8*g* (Table S2). The B−D bonds are 1.05~1.29 Å in length, which is in good agreement with B−H in $NaBH_4$ and $LiBH_4$.[25,26] The high multiplicity sites, the low occupying ratio, and the large anisotropic temperature factors (B value in Table S2) of D atoms may reflect the high rotation of D around B atom rather than the fixed D positions even at 300 K.

Differential scanning calorimetry (DSC) is applied to study the thermal stability of Na_3OBH_4 (Figure 3a). The

DOI: 10.1021/jacs.9b01746
J. Am. Chem. Soc. 2019, 141, 5640−5644

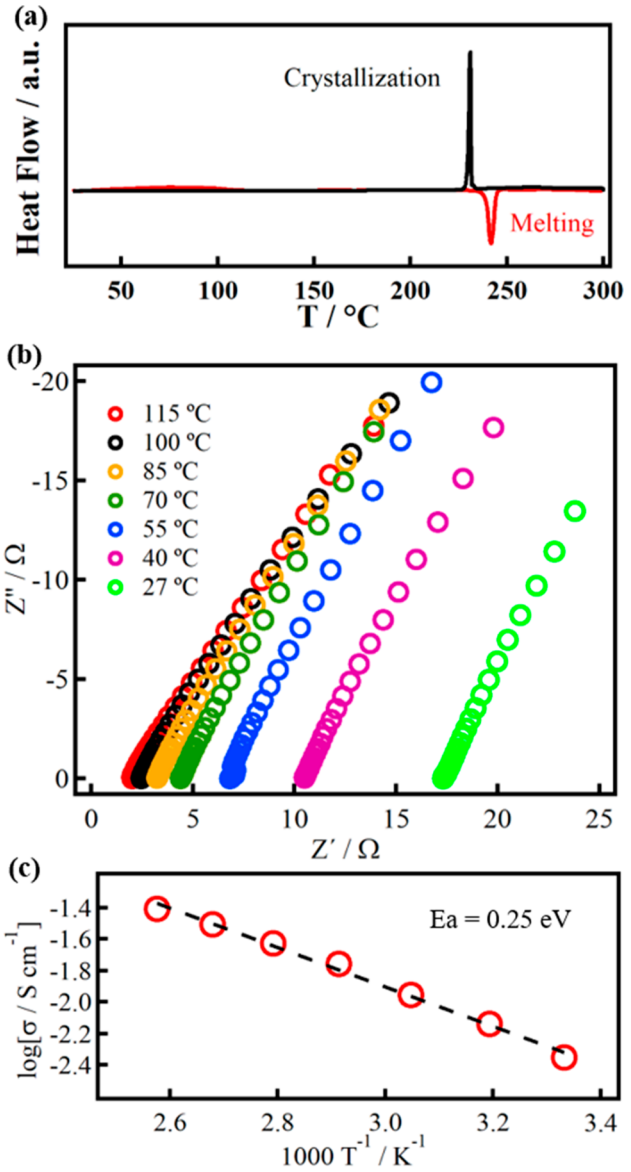

Figure 3. (a) Differential scanning calorimetry (DSC) of Na_3OBH_4; (b) Nyquist plots of hot-pressed Na_3OBH_4 pellet in the temperature range of 300−390 K and (c) corresponding Arrhenius conductivity plot.

endothermic/exothermic peaks during heating/cooling represent the melting and crystallization processes. The melting point is about 240 °C, which is close to that of Na_3OX (X = Cl, Br, I).[19] Except for the melting/crystallization peaks, no peaks related to phase transition or A-site (X sites in Na_3OX, X = Br/I) ordering/disordering are observed in the DSC curves.[19] Only one A-site (the site for BH_4 anion) in Na_3OBH_4 is also supported by structural information (Table S2) and the ^{11}B solid state NMR spectrum (Figure S3). The ionic conductivity of Na_3OBH_4 is measured by AC impedance based on cold-pressed powders and hot-pressed pellets. The cold-pressed powders show large resistance (Figure S5), which may result from the grain-boundary resistance from its oxide nature although borohydrides have good formability.[23,27,28] Based on the DSC results, the pellet is hot-pressed under 100 °C that is a bearable temperature for the homemade die. Hot-press has largely densified the pellet (density in Table S3 and SEM in Figure S6). Figure 3b shows the Nyquist plots of hot-pressed Na_3OBH_4 pellet in the temperature range of 300−390 K. The Nyquist plot for each temperature contains only spike attributed to electrolyte/Au blocking electrode interface, which indicates pure ionic conduction characteristics of antiperovskite Na_3OBH_4. The total ionic conductivities are calculated based on the intercept to the real axis. The calculated ionic conductivity at room temperature (300 K) is 4.4×10^{-3} S cm^{-1}, and 1.1×10^{-2} S cm^{-1} at 328 K, which is comparable to liquid electrolyte and higher than those of NASICON-type ceramics and sulfides (Figure 4).[6−10] The electronic

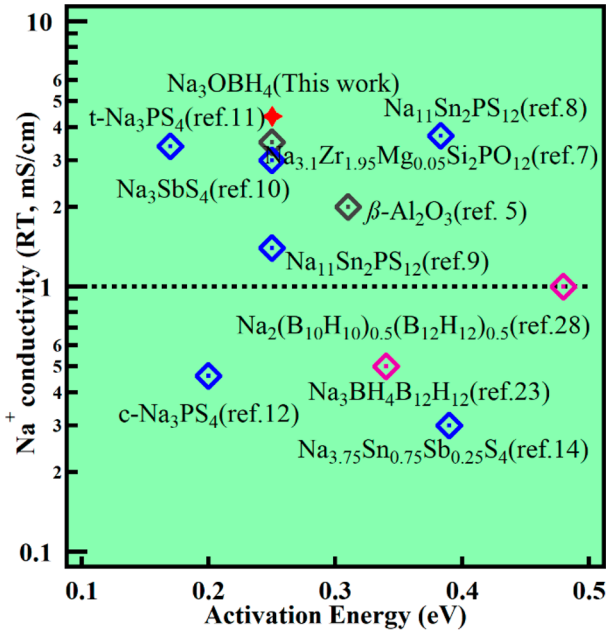

Figure 4. Sodium ionic conductivity and the activation energy of a variety of ionic conductors.

conductivity is detected to be ~10^{-7} S cm^{-1} (DC polarization measurements in Figure S7), which is 4 orders of magnitude lower than the ionic conductivity measured by AC impedance. Therefore, the contribution of electron conduction to total conductivity is negligible. The Arrhenius conductivity plot in the temperature range of 300−390 K is shown in Figure 3c. The calculated activation energy for Na^+ conduction in Na_3OBH_4 based on Arrhenius equation is 0.25 eV, which is comparable with other superionic conductors (Figure 4).

The ionic conductivity of Li/Na antiperovskites is facilitated by defects in structures,[29] such as the Na vacancies.[30] The high concentration of Na vacancy in Na_3OBH_4/Na_3OBD_4 (Table S2) that may be generated during processing is one reason for the high ionic conductivity. The substitution of Na^+ by Ca^{2+} to further increase vacancy density is conducted. However, Ca^{2+} cannot be introduced into Na_3OBH_4 antiperovskite (Figure S8). Notably, the ionic conductivity is 4 orders of magnitude higher than that of Na_3OX (X = Cl, Br, I). Given the same antiperovskite structure and the close lattice parameters to Na_3OBr, the enhancement in ionic conductivity may result from the specific structure of Na_3OBH_4. The ^{23}Na NMR signs (Figure 2) illustrate that Na_3OBr may slightly distort from the cubic antiperovskite structure. Both the solid state NMR spectrum and refinement results demonstrate the cubic antiperovskite structure without Na site distortion in Na_3OBH_4, which can afford an anisotropic 3D pathways via vacancies.[31] Additionally, the chemical shift of ^{23}Na in

DOI: 10.1021/jacs.9b01746
J. Am. Chem. Soc. 2019, 141, 5640−5644

Na_3OBH_4 suggests a lower electronic cloud density around Na in Na_3OBH_4 than that in Na_3OBr.

The neutron diffraction results suggest the rotation of BH_4 group and possible relation of the rotation and Na diffusion. To further clarify the mechanism underlying efficient ionic conductivity in Na_3OBH_4, we have also performed in-depth first-principles calculations. The Na ion migration barriers in Na_3OX (X = Br and BH_4) are calculated by using the climbing image nudged elastic band (CI-NEB) approach with a $2 \times 2 \times 1$ supercell with one Na vacancy. When using optimized crystal structures, the calculated Na migration barrier in Na_3OBH_4 is about 0.1 eV lower than that in Na_3OBr (0.39 vs 0.48 eV). We also find that the nearly free rotation (with a calculated rotation barrier of about 0.02 eV) of BH_4 plays a crucial role for the lower Na migration barrier in Na_3OBH_4 (Table S5). Fixing BH_4 during the Na migration leads to a much higher barrier (0.55 eV). To further model the Na ion migration at finite temperature, we have also performed *ab initio* molecular dynamics (AIMD) simulations. Within a period of 40 ps simulation after 10 ps for equilibration, the number of successful Na migration is 0 (1) in Na_3OBr, and 2 (5) in Na_3OBH_4 at T = 700 (900) K, (Table S6) which clearly indicates that Na migration is significantly more efficient in Na_3OBH_4 than in Na_3OBr. Inspired by these results for Na, the synthesis of the Li-counterpart, Li_3OBH_4 has been attempted, but fails perhaps because the synthesis is solid-state reaction rather than the recommended high pressures.[20]

In summary, Na_3OBH_4 has been successfully synthesized by a facile solid-state reaction. Solid state NMR and XRD results reveal that Na_3OBH_4 crystallizes into the cubic antiperovskite structure without distortion. Na_3OBH_4 exhibits the ionic conductivity of 4.4×10^{-3} S cm^{-1} at room temperature and 1.1×10^{-2} S cm^{-1} at 328 K. The rotation of BH_4 can facilitate the Na migration. This work will ignite the investigation on cluster anions based superionic conductors, especially their conduction mechanism. Studies on further optimization and corresponding all-solid-state sodium batteries are underway.

■ ASSOCIATED CONTENT

Supporting Information

The Supporting Information is available free of charge on the ACS Publications website at DOI: 10.1021/jacs.9b01746.

Experimental details, supplementary results such as structures analysis and calculations (PDF)

■ AUTHOR INFORMATION

Corresponding Authors

*xiejia@hust.edu.cn

*jianghchem@pku.edu.cn

ORCID

Jiwen Feng: 0000-0002-9691-8574

Hong Jiang: 0000-0003-3187-2023

Jia Xie: 0000-0002-8731-295X

Notes

The authors declare no competing financial interest.

■ ACKNOWLEDGMENTS

This work is supported by the National Basic Research Program of China (973 Program, 2015CB258400), the Program for HUST Interdisciplinary Innovation Team (2015ZDTD021), National Natural Science Foundation of China (21673005 and 21621061), the China Postdoctoral Science Foundation Grant (2017M622422), and China Postdoctoral Science Foundation (BX201700003). The authors gratefully acknowledge the Analytical and Testing Center of HUST and High-Performance Computing Platform of Peking University for allowing us to use their facilities.

■ REFERENCES

(1) Kim, J.-J.; Yoon, K.; Park, I.; Kang, K. Progress in the Development of Sodium-Ion Solid Electrolytes. *Small Methods.* **2017**, *1*, 1700219.

(2) Zhao, C.; Liu, L.; Qi, X.; Lu, Y.; Wu, F.; Zhao, J.; Yu, Y.; Hu, Y.-S.; Chen, L. Solid-State Sodium Batteries. *Adv. Energy. Mater.* **2018**, *8*, 1703012.

(3) Yabuuchi, N.; Kubota, K.; Dahbi, M.; Komaba, S. Research Development on Sodium-Ion Batteries. *Chem. Rev.* **2014**, *114*, 11636−11682.

(4) Lu, Y.; Li, L.; Zhang, Q.; Niu, Z.; Chen, J. Electrolyte and Interface Engineering for Solid-State Sodium Batteries. *Joule.* **2018**, *2*, 1747−1770.

(5) Wenzel, S.; Leichtweiss, T.; Weber, D. A.; Sann, J.; Zeier, W. G.; Janek, J. Interfacial Reactivity Benchmarking of the Sodium Ion Conductors Na_3PS_4 and Sodium *ß*-Alumina for Protected Sodium Metal Anodes and Sodium All-Solid-State Batteries. *ACS Appl. Mater. Interfaces* **2016**, *8*, 28216−28224.

(6) Ma, Q.; Guin, M.; Naqash, S.; Tsai, C.-L.; Tietz, F.; Guillon, O. Scandium-Substituted $Na_3Zr_2(SiO_4)_2(PO_4)$ Prepared by a Solution Assisted Solid-State Reaction Method as Sodium-Ion Conductors. *Chem. Mater.* **2016**, *28*, 4821−4828.

(7) Song, S.; Duong, H. M.; Korsunsky, A. M.; Hu, N.; Lu, L. A Na+ Superionic Conductor for Room-Temperature Sodium Batteries. *Sci. Rep.* **2016**, *6*, 32330.

(8) Duchart, M.; Ruschewitz, U.; Adams, S.; Dehnen, S.; Roling, B. Vacancy-Controlled Na^+ Superion Conduction in $Na_{11}Sn_2PS_{12}$. *Angew. Chem., Int. Ed.* **2018**, *57*, 1351−1355.

(9) Zhang, Z.; Ramos, E.; Lalère, F.; Assoud, A.; Kaup, K.; Hartman, P.; Nazar, L. F. $Na_{11}Sn_2PS_{12}$: a New Solid State Sodium Superionic Conductor. *Energy Environ. Sci.* **2018**, *11*, 87−93.

(10) Zhang, L.; Zhang, D.; Yang, K.; Yan, X.; Wang, L.; Mi, J.; Xu, B.; Li, Y. Vacancy-Contained Tetragonal Na_3SbS_4 Superionic Conductor. *Adv. Sci.* **2016**, *3*, 1600089.

(11) Takeuchi, S.; Suzuki, K.; Hirayama, M.; Kanno, R. Sodium Superionic Conduction in Tetragonal Na_3PS_4. *J. Solid State Chem.* **2018**, *265*, 353−358.

(12) Hayashi, A.; Noi, K.; Tanibata, N.; Nagao, M.; Tatsumisago, M. High Sodium Ion Conductivity of Glass-Ceramic Electrolytes with Cubic Na_3PS_4. *J. Power Sources* **2014**, *258*, 420−423.

(13) Hayashi, A.; Noi, K.; Sakuda, A.; Tatsumisago, M. Superionic Glass-Ceramic Electrolytes for Room-Temperature Rechargeable Sodium Batteries. *Nat. Commun.* **2012**, *3*, 856.

(14) Heo, J. W.; Banerjee, A.; Park, K. H.; Jung, Y. S.; Hong, S.-T. New Na-Ion Solid Electrolytes $Na_{4-x}Sn_{1-x}Sb_xS_4$ ($0.02 \leq x \leq 0.33$) for All-Solid-State Na-Ion Batteries. *Adv. Energy Mater.* **2018**, *8*, 1702716.

(15) Tang, H.; Deng, Z.; Lin, Z.; Wang, Z.; Chu, I.-H.; Chen, C.; Zhu, Z.; Zheng, C.; Ong, S. P. Probing Solid-Solid Interfacial Reactions in All-Solid-State Sodium-Ion Batteries with First-Principles Calculations. *Chem. Mater.* **2018**, *30*, 163−173.

(16) Zhao, Y.; Daemen, L. L. Superionic conductivity in Lithium-Rich Anti-Perovskites. *J. Am. Chem. Soc.* **2012**, *134*, 15042−15047.

(17) Emly, A.; Kioupakis, E.; Van der Ven, V. A. Phase Stability and Transport Mechanisms in Antiperovskite Li_3OCl and Li_3OBr Superionic Conductors. *Chem. Mater.* **2013**, *25*, 4663−4670.

(18) Lü, X.; Wu, G.; Howard, J. W.; Chen, A.; Zhao, Y.; Daemen, L. L.; Jia, Q. Li-rich Anti-perovskite Li_3OCl Films with Enhanced Ionic Conductivity. *Chem. Commun.* **2014**, *50*, 11520−11522.

(19) Wang, Y.; Wang, Q.; Liu, Z.; Zhou, Z.; Li, S.; Zhu, J.; Zou, R.; Wang, Y.; Lin, J.; Zhao, Y. Structural Manipulation Approaches

DOI: 10.1021/jacs.9b01746
J. Am. Chem. Soc. 2019, 141, 5640−5644

towards Enhanced Sodium Ionic Conductivity in Na-rich Antiperovskites. *J. Power Sources* **2015**, *293*, 735−740.
(20) Fang, H.; Wang, S.; Liu, J.; Sun, Q.; Jena, P. Superhalogen-based Lithium Superionic Conductors. *J. Mater. Chem. A* **2017**, *5*, 13373−13381.
(21) Fang, H.; Jena, P. Li-rich antiperovskite Superionic Conductors based on Cluster Ions. *Proc. Natl. Acad. Sci. U. S. A.* **2017**, *114*, 11046−11051.
(22) Fang, H.; Jena, P. Sodium Superionic Conductors Based on Clusters. *ACS Appl. Mater. Interfaces* **2019**, *11*, 963−972.
(23) Sadikin, Y.; Brighi, M.; Schouwink, P.; černý, R. Superionic Conduction of Sodium and Lithium in Anion-Mixed hydroborates $Na_3BH_4B_{12}H_{12}$ and $(Li_{0.7}Na_{0.3})_3BH_4B_{12}H_{12}$. *Adv. Energy. Mater.* **2015**, *5*, 1501016.
(24) Li, Z.; Yang, M.; Park, J.-S.; Wei, S.-H.; Berry, J. J.; Zhu, K. Stabilizing Perovskite Structures by Tuning Tolerance Factor: Formation of Formamidinium and Cesium Lead Iodide Solid-State Alloys. *Chem. Mater.* **2016**, *28*, 284−292.
(25) Filinchuk, Y.; Hagemann, H. Structure and Properties of $NaBH_4{\cdot}2H_2O$ and $NaBH_4$. *Eur. J. Inorg. Chem.* **2008**, *2008*, 3127−3133.
(26) Soulié, J. P.; Renaudin, G.; černý, R.; Yvon, K. Lithium boro-hydride $LiBH_4$ I. Crystal Structure. *J. Alloys Compd.* **2002**, *346*, 200−205.
(27) Maekawa, H.; Matsuo, M.; Takamura, H.; Ando, M.; Noda, Y.; Karahashi, T.; Orimo, S.-I. Halide-Stabilized $LiBH_4$, a Room-Temperature Lithium Fast-Ion Conductor. *J. Am. Chem. Soc.* **2009**, *131*, 894−895.
(28) Yoshida, K.; Sato, T.; Unemoto, A.; Matsuo, M.; Ikeshoji, T.; Udovic, T. J.; Orimo, S.-I. Fast Sodium Ionic Conduction in $Na_2B_{10}H_{10}$-$Na_2B_{12}H_{12}$ Pseudo-Binary Complex Hydride and Application to a Bulk-Type All-Solid-State Battery. *Appl. Phys. Lett.* **2017**, *110*, 103901.
(29) Yang, Q.; Li, C. Li Metal Batteries and Solid State Batteries Benefiting from Halogen-based Strategies. *Energy Storage Mater.* **2018**, *14*, 100−117.
(30) Nguyen, H.; Hy, H.; Wu, E.; Deng, Z.; Samiee, M.; Yersak, T.; Luo, J.; Ong, S. P.; Meng, Y. S. Experimental and Computational Evaluation of a Sodium-Rich Anti-Perovskite for Solid State Electrolytes. *J. Electrochem. Soc.* **2016**, *163*, A2165−A2171.
(31) Zhu, J.; Wang, Y.; Li, S.; Howard, J. W.; Neuefeind, J.; Ren, Y.; Wang, H.; Liang, C.; Yang, W.; Zou, R.; Jin, C.; Zhao, Y. Sodium Ion Transport Mechanisms in Antiperovskite Electrolytes Na_3OBr and Na_4OI_2: An in Situ Neutron Diffraction Study. *Inorg. Chem.* **2016**, *55*, 5993−5998.

DOI: 10.1021/jacs.9b01746
J. Am. Chem. Soc. 2019, 141, 5640−5644